

Block-copolymer healing of simple defects in a chemoepitaxial template

Paul N. Patrone,^{1,2,3,4} Gregg M. Gallatin^{1,5}

¹Center for Nanoscale Science and Technology, National Institute of Standards and Technology, Gaithersburg, Maryland 20899-1070 USA

²Department of Physics, University of Maryland, College Park, Maryland 20742-4111 USA

³Institute for Research in Electronics and Applied Physics, University of Maryland, College Park, Maryland 20742-4111 USA

⁴ Condensed Matter Theory Center, University of Maryland, College Park, Maryland 20732-4111

⁵ Applied Math Solutions LLC, Newtown, Connecticut 06470

ABSTRACT

Using the Leibler-Ohta-Kawasaki (LOK) phase-field model of block copolymers (BCPs), we characterize how a chemoepitaxial template with parallel lines of arbitrary width affects the BCP microdomain shape. We apply boundary conditions that account for the interactions of the polymers with the templated substrate and a neutral top-coat. We derive formulas for the monomer density and the microdomain interface profile of periodic, lamellar BCP melts whose template lines are wider or narrower than the bulk microdomain width. For such systems, our analysis (i) shows that mass conservation causes the microdomain interfaces to oscillate about their bulk positions and (ii) determines the length scale λ over which these oscillations decay away from the substrate.

1. INTRODUCTION

In recent years, interest in self-assembling block copolymers (BCPs) has increased dramatically, due in large part to their potential applications in the semiconductor industry. One of the key properties that makes BCPs promising is their ability self-assemble into microdomains whose size, shape, and spacing are the same as or smaller than features found in modern microprocessors.^{1,2} Moreover, in systems where a chemical (or chemoepitaxial) template induces long range order in the polymer melt, BCPs can assemble into the desired pattern, even though the template itself may have defects and line edge roughness (LER).^{3–6} Because this “healing” process is so crucial to high-fidelity pattern transfer in lithography, it is important to understand in detail how defects in the template affect the BCP microdomains. (Note that BCPs also have intrinsic LER coming from thermal fluctuations.⁷)

In this work, our goal is to characterize how a chemoepitaxial template with parallel lines of arbitrary width affects the BCP microdomain shape. To this end, we study a version of the Leibler-Ohta-Kawasaki (LOK) phase-field Hamiltonian^{8,9} that explicitly accounts for interactions of the polymers with the substrate and a neutral top-coat. Using this model, we derive expressions for (i) the monomer density and (ii) the microdomain interface profiles for strongly segregated, lamellar systems with periodically spaced, parallel template lines whose width is greater than that of the bulk microdomains; see Figs. 1 and 2. Our analysis, in particular, highlights the crucial role that mass conservation can play in determining the shape of thin film microdomains.

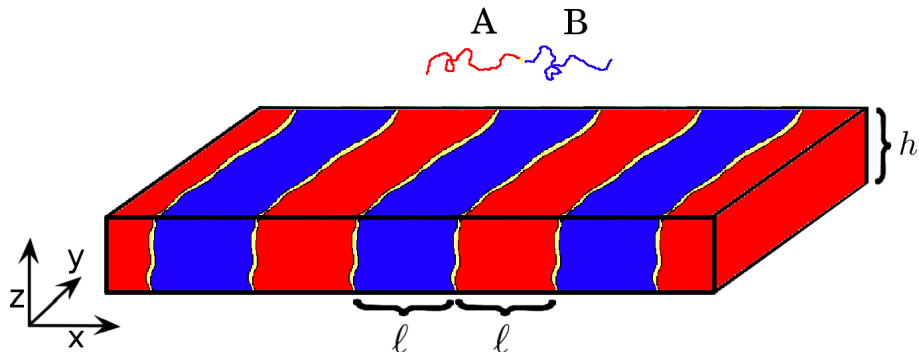


Figure 1. A BCP melt in the strong segregation regime (SSR). The width of A (blue) and B (red) microdomains is ℓ , while h is the thickness of the melt. The yellow region separating the A and B microdomains is much smaller than ℓ .

Top View of Template Side View of BCPs

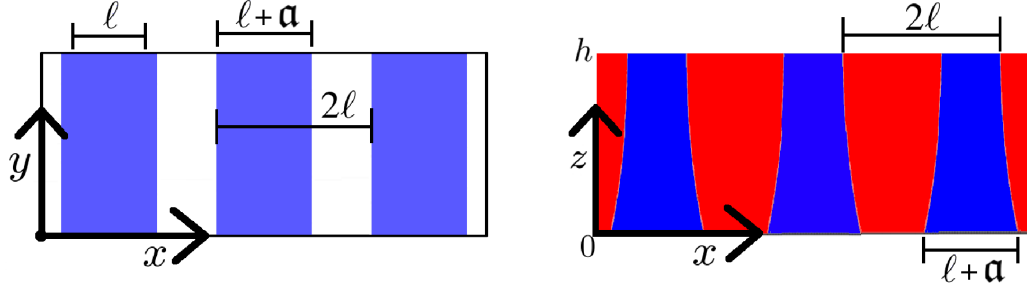


Figure 2. Chemoepitaxial template (left) and assembled block copolymer microdomains (right). The template is a periodic array of straight lines that are parallel to the y -axis. The A monomers (blue) assemble into microdomains over top of the template lines (right).

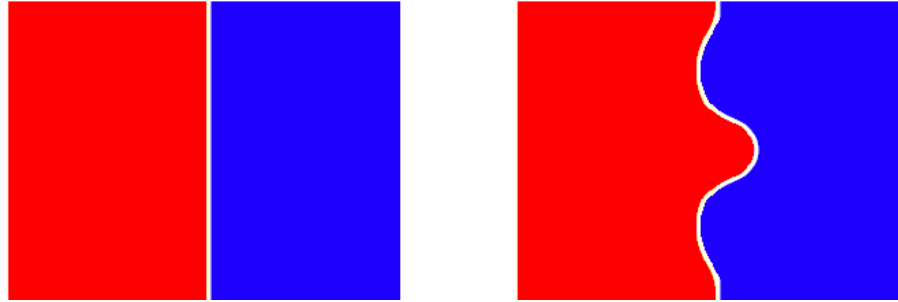


Figure 3. Two interface geometries. Deformation of the interface occurs by redistributing the (incompressible) mass of red and blue polymers. The area of red (and blue) is the same in both figures.

The key idea of our analysis is to exploit the fact that changing the relative number of monomers near a microdomain interface causes it to deform; see Fig. 3. Using this fact, we are able to recast the LOK Hamiltonian into an equation for the interfaces by defining them in terms of an integral of the monomer density. Critically, this transformation reduces the *non-linear* partial differential equation (PDE) for the monomer density into a constant-coefficient *linear* differential equation for the interface profiles, which can be solved exactly.

Similar questions have been addressed by Refs. [5] and [6], who relied heavily on computer simulations. While such methods are useful for studying complex systems, there is considerable computational overhead associated with exploring the parameter space that is available for industrial applications. Hence, our work is motivated in part by the need for simple models that capture the essential physics of BCPs over a range of material parameters.

The starting point of our analysis is a variation of the phase-field model originally developed by Leibler, Ohta, and Kawasaki (LOK),^{8,9} which gives the energy $\mathcal{H}[\phi]$ of a polymer melt as a function of the relative density (defined below) of monomer species. In their original work, they determined that the lowest energy configuration (for equal molecular weights of the two monomer types) was indeed a lamellar, phase-separated system with planar interfaces separating microdomains. In adapting their model to our needs, we must (i) determine boundary conditions that account for interactions of the polymer with the substrate and top-coat, and (ii) minimize the resulting energy functional in order to find the interface profiles.

Our choice of model is driven in large part by consideration of the features that we wish to describe. On a microscopic scale, individual polymers exhibit complicated geometries and foldings, which are adequately described by Gaussian chain models, molecular dynamics, and Monte Carlo simulations,^{10–13} for example. However, for polymer melts whose domains span tens of nanometers, the computational expense of using such models becomes insurmountable, owing simply to the number of particles that must be taken into account. Moreover, at such length scales, one typically wishes to study mesoscopic features (such as the microdomain interface positions)

of the melt as a whole, as opposed to the structure of individual molecules. Phase field models therefore enter as computationally tractable alternatives that (i) permit study of quantities relevant at the nanometer length scale, while (ii) coarse-graining microscopic features that otherwise render computation difficult. In our present analysis, we use the LOK phase-field model since it is analytically tractable, and recent studies suggest that it could be well suited to describe fluctuations in technologically relevant systems.^{7,14,15}

We end this section by summarizing notation that will be used throughout the remainder of the text:

i) a is the Kuhn statistical length, which measures the average distance between two adjacent monomers. This length is considered small relative to the system size.

ii) χ denotes the dimensionless Flory-Huggins parameter, which characterizes the repulsion between different monomer species.

iii) N denotes the index of polymerization, i.e. the number of monomers in a single chain.

iv) f is the (normalized) molecular weight of A monomers; $(1 - f)$ is the molecular weight of B monomers.

v) $\phi(\mathbf{x}) = \phi_A(\mathbf{x}) - \phi_B(\mathbf{x})$ denotes the relative density of A monomers $[\phi_A(\mathbf{x})]$ and B monomers $[\phi_B(\mathbf{x})]$. We choose the normalization $0 \leq \phi_A(\mathbf{x}), \phi_B(\mathbf{x}) \leq 1$ and impose the incompressibility condition $\phi_A(\mathbf{x}) + \phi_B(\mathbf{x}) = 1$, so that $-1 \leq \phi \leq 1$.

v) The symbol Ω denotes the volume of the system, whereas \mathcal{V} denotes a unit volume.

2. SYSTEM AND MAIN RESULTS

In this section, we characterize how a chemoepitaxial template with parallel lines of arbitrary width affects the BCP microdomain shape. In particular, we (i) give formulas for the monomer density profile and the microdomain interface profiles, and (ii) determine a length scale λ over which the template affects the melt in a direction perpendicular to the substrate.

Consider a lamellar, diblock copolymer melt in the strong-segregation regime (SSR); see Fig. 1. For simplicity, we take the molecular weights of the A and B subchains to be equal (i.e. $f = 1/2$) and denote ℓ as the bulk width of A (or B) domains. Since the system is in the SSR, the boundaries (yellow regions in Fig. 1) between the A and B domains are small compared to ℓ . The parameter h denotes the height of the melt, and we assume that the system is infinite in the x and y directions.[†] We further assume that straight template lines are patterned onto the substrate in a direction parallel to the y -axis and with a periodicity 2ℓ . These lines, which attract A monomers (for example), have a width $\ell + a$ (where a is not to be confused with the Kuhn length a ; cf. Fig. 2). Because of their attraction to the template, the A monomers assemble into microdomains over top of the template lines; see Fig. 2.

In a unit cell $0 \leq x \leq 2\ell$ and $0 \leq z \leq h$, we assume that the density ϕ can be written in the form^{7–9}

$$\phi(x, z) = -1 + \tanh \left[\frac{x - (\ell/2) + (f(z)/2)}{\sqrt{2}\xi} \right] - \tanh \left[\frac{x - (3\ell/2) - (f(z)/2)}{\sqrt{2}\xi} \right], \quad (1)$$

where $\xi := a/\sqrt{f(1-f)\chi}$ and $f(z)$ is an unknown function. In Section 4 we determine that

$$\begin{aligned} \frac{f(z)}{a} &= \left[\frac{\cos(2h/\lambda) - \sin(2h/\lambda) - e^{-2h/\lambda}}{e^{2h/\lambda} - 4 \cos(h/\lambda) \sin(h/\lambda) - e^{-2h/\lambda}} \right] e^{z/\lambda} \cos[z/\lambda] + \left[\frac{\cos(2h/\lambda) + \sin(2h/\lambda) - e^{-2h/\lambda}}{e^{2h/\lambda} - 4 \cos(h/\lambda) \sin(h/\lambda) - e^{-2h/\lambda}} \right] e^{z/\lambda} \sin[z/\lambda] \\ &- \left[\frac{\cos(2h/\lambda) + \sin(2h/\lambda) - e^{2h/\lambda}}{e^{2h/\lambda} - 4 \cos(h/\lambda) \sin(h/\lambda) - e^{-2h/\lambda}} \right] e^{-z/\lambda} \cos[z/\lambda] + \left[\frac{\cos(2h/\lambda) - \sin(2h/\lambda) - e^{2h/\lambda}}{e^{2h/\lambda} - 2 \sin(h/\lambda) - e^{-2h/\lambda}} \right] e^{-z/\lambda} \sin[z/\lambda], \end{aligned} \quad (2)$$

where

$$\lambda = aN^{1/2} \left[\frac{f(1-f)}{27} \right]^{1/4} \quad (3)$$

[†]Our analysis is trivially generalized to systems that are finite in the x and y direction by converting the appropriate integrals to sums.

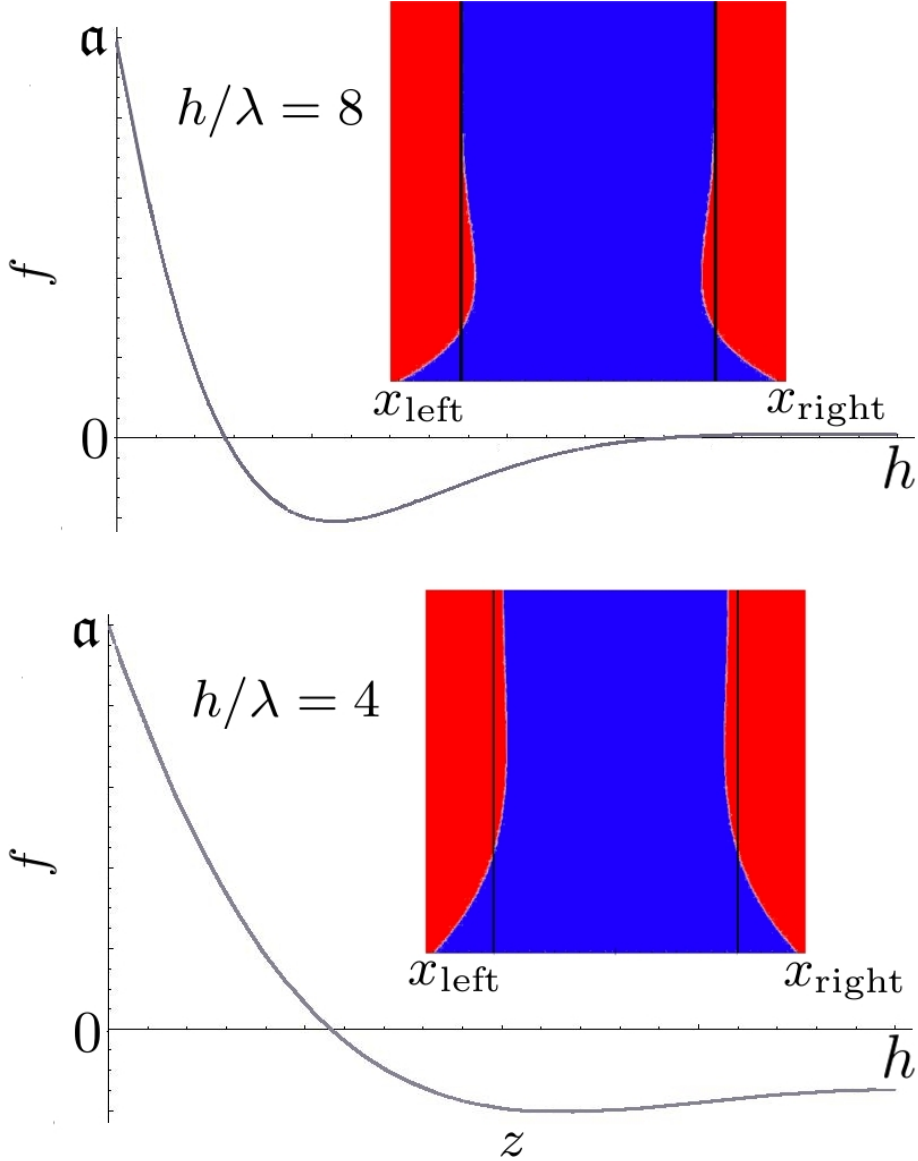


Figure 4. The function $f(z)$ for arbitrary α when $h/\lambda = 8$ (top) and $h/\lambda = 4$ (bottom). The insets show the polymer melts and the positions of x_{left} and x_{right} when $\alpha = \ell/2$. The vertical black lines denote the mean interface position.

determines the length scale over which the substrate affects the melt. For fixed z , Eq. (1) is (approximately) a square wave whose maximum and minimum are ± 1 ; physically, this density corresponds to strongly segregated microdomains of A (+) and B (-) monomers. Each microdomain has a width $\ell \pm f(z)$, and the interface separating microdomains has a width $2\sqrt{2}\xi$.

The microdomain interfaces are curves $x = x(z)$:

$$x_{\text{left}}(z) = \frac{\ell}{2} + 2\ell n - \frac{f(z)}{2}, \quad (4)$$

$$x_{\text{right}}(z) = \frac{3\ell}{2} + 2\ell n + \frac{f(z)}{2}, \quad (5)$$

where the A polymers are confined between x_{left} and x_{right} ; see Fig. 4.

To understand the behavior of $f(z)$ (and consequently x_{left} and x_{right}), it is sufficient to look at the limit $h \gg \lambda$ (i.e. a thick film). In this limit, the coefficients multiplying the $e^{z/\lambda}$ are exponentially small, and $f \approx \alpha e^{-z/\lambda} [\cos(z/\lambda) - \sin(z/\lambda)]$. The interfaces oscillate around their bulk (or mean) positions (corresponding to $f = 0$), and these oscillations decay over the length scale λ . For $N = 300$ (roughly corresponding to $\ell = 8$ nm), $a = 1$ nm, and $f = 1/2$ (for example), one finds $\lambda \approx 5$ nm, which is nominally a sizable fraction of the resist thickness required for industrial applications.

Note that λ , and consequently f , only depend on the radius of gyration $R_g \sim N^{1/2}$, and not χ ; this suggests that the microdomain shape is determined by minimizing the part of the energy associated with polymer bending (and not the A-B repulsive interaction). Consistent with this idea, it is also possible to show that f satisfies the condition $\int_0^h f(z) dz = 0$. This equation can be interpreted as a statement of mass conservation in the following sense: the total number of A monomers in a given microdomain is independent of the width of the template $\ell + \alpha$, *but the position of the monomers does depend on α via f* . In other words, deforming an interface can only occur by “shifting mass” in a way that conserves the total number of A monomers; see Figs. 3 and 4.*

Importantly, we predict that substrate effects could become *more important* as feature sizes decrease. Fixing a , we note that the microdomain width $\ell \sim N^{2/3}$, while $\lambda \sim N^{1/4}$. Assuming that the film height $h \sim \ell$, we see that the film thickness will decrease much faster than the length scale over which the substrate affects the system. Physically this observation has a simple interpretation: shorter polymers have less degrees of freedom that allow the BCP morphology to relax away from the substrate, i.e. polymers effectively become more rigid as they shorten.

3. PHASE-FIELD MODEL

We model the system described in Sec. 2 with a variation of the Leibler-Ohta-Kawasaki energy functional

$$\mathcal{H}[\phi] = \frac{k_B T \chi}{\mathcal{V}} \int_{\mathcal{V}} dV \left\{ \frac{\xi^2}{2} (\nabla \phi)^2 - \frac{\phi^2}{2} + \frac{\phi^4}{4} + \frac{\varsigma}{2} \int_{\Omega} dV' \phi(\mathbf{r}) g(\mathbf{r}, \mathbf{r}') \phi(\mathbf{r}') \right\}, \quad (6)$$

$$\xi^2 := \frac{a^2}{3f(1-f)\chi} \quad \varsigma := \frac{36}{f^2(1-f)^2 a^2 \chi \mathcal{N}^2}. \quad (7)$$

The product $k_B T$ is Boltzmann’s constant times the temperature, and the function $g(\mathbf{r}, \mathbf{r}')$ is the Green’s function of the Laplacian. We assume that $\partial_z g = 0$ when $z = 0$ and $z = h$, so that g takes the form

$$g(\mathbf{r}, \mathbf{r}') = \int_{-\infty}^{\infty} dk_x \int_{-\infty}^{\infty} dk_y \frac{e^{ik_x(x-x')+ik_y(y-y')}}{(k_x^2 + k_y^2)(2\pi)^2 h} + 2 \sum_{k_z} \int_{-\infty}^{\infty} dk_x \int_{-\infty}^{\infty} dk_y \frac{e^{ik_x(x-x')+ik_y(y-y')} \cos(k_z z) \cos(k_z z')}{(k_x^2 + k_y^2 + k_z^2)(2\pi)^2 h}, \quad (8)$$

where $k_z = \pi n/h$, $n = 1, 2, \dots$.

Equation (6) is an *effective* field theory that views the melt from a coarse-grained perspective. Individual polymers are not considered; rather the configuration of the system is accounted for through the relative density ϕ of A and B polymers (which is a continuous function). Interfaces between A and B domains are represented by *boundary layers* (cf. Fig. 5), i.e. narrow regions in which the density ϕ changes rapidly. The parameter ξ determines the boundary layer thickness and is generally considered small in the sense $\xi \ll \ell$ whenever $\chi \mathcal{N} \gg 1$, which corresponds to the system being in the SSR.

Equation (6) is supplemented by boundary conditions for the density ϕ . We assume that (i) the chemical template is strongly attracted to the A monomers, and (ii) the microdomain interface is pinned to the edge of the chemical template. Mathematically this condition is expressed via

$$\phi(x, 0) = -1 + \tanh \left[\frac{x - (\ell/2) + (\alpha/2)}{\sqrt{2}\xi} \right] - \tanh \left[\frac{x - (3\ell/2) - (\alpha/2)}{\sqrt{2}\xi} \right]. \quad (9)$$

*We write “shifting mass” in quotes to emphasize that this description is not technically consistent with our approach, since we do not consider a time-dependent problem.

On the $z = h$ plane, we allow the microdomain interface to find the position that minimizes Eq. (6) (i.e. ϕ satisfies the *natural* boundary condition at $z = h$). We therefore consider a $\hat{\phi} + \delta\phi$ such that (i) $\hat{\phi}$ minimizes \mathcal{H} , (ii) $\delta\phi = 0$ on $z = 0$, (iii) $\delta\phi \rightarrow 0$ as $x, y \rightarrow \pm\infty$, and (iv) $\delta\phi \neq 0$ on $z = h$. Setting the first variation of \mathcal{H} equal to zero yields

$$\begin{aligned} 0 &= \int_{\mathcal{V}} dV \left\{ \xi^2 \nabla \hat{\phi} \cdot \nabla \delta\phi + (\hat{\phi}^3 - \hat{\phi}) \delta\phi + \varsigma \int_{\Omega} dV' \delta\phi(\mathbf{r}) g(\mathbf{r}, \mathbf{r}') \hat{\phi}(\mathbf{r}') \right\}, \\ &= \int_{\mathcal{V}} dV \left\{ (-\xi^2 \nabla^2 \hat{\phi} + \hat{\phi}^3 - \hat{\phi}) \delta\phi + \varsigma \int_{\Omega} dV' \delta\phi(\mathbf{r}) g(\mathbf{r}, \mathbf{r}') \hat{\phi}(\mathbf{r}') \right\} + \int_{z=h} dS \delta\phi \partial_z \hat{\phi}. \end{aligned} \quad (10)$$

In order for Eq. (10) to be true, we require that $\hat{\phi}$ solve

$$0 = -\xi^2 \nabla^2 \hat{\phi} - \hat{\phi} + \hat{\phi}^3 + \varsigma \int_{\Omega} dV' g(\mathbf{r}, \mathbf{r}') \hat{\phi}(\mathbf{r}'), \quad (11)$$

subject to Eq. (9) and the boundary condition $\partial_z \hat{\phi}|_{z=h} = 0$. Equation (10) differs from the original work by Leibler, Ohta, and Kawasaki insofar as their model assumed that the melt is infinite in all three directions, whereas ours does not.

4. SOLVING FOR THE MONOMER DENSITY

In this section, we describe how to solve Eq. (11) for Eqs.(2)–(5).

We begin by assuming that $\hat{\phi}$ is given by Eq. (1), where $f(z)$ is an unknown function. Physically, this amounts to the assumption that the density profile is everywhere the same as for a bulk system, but with interface positions shifted by $f(z)/2$. We require that $f(h) \rightarrow 0$ when $h \rightarrow \infty$ (i.e. when the film becomes infinitely thick), so that our solution asymptotically approaches the LOK bulk solution far from the substrate.⁸ Consequently, we identify ℓ as the microdomain width of a bulk system. Since the system is translationally invariant in the y -direction, we take $\hat{\phi}$ to be a function of only x and z .

In order to find the interface profiles, we first note that in any plane $z = z_0$, $f(z_0) \neq 0$ increases the number of A monomers by an amount proportional to $f(z_0)$ while decreasing the B monomers by the same amount (or vice versa); i.e. f increases (or decreases) the width of each microdomain (see Fig. 5). Moreover, since ϕ quickly approaches ± 1 away from each microdomain interface, we identify

$$f(z) \approx \frac{1}{2} \int_0^{2\ell} \phi(x, z) dx \quad (12)$$

$$= \lim_{n \rightarrow \infty} \frac{1}{2(2n+1)} \int_{-2n\ell}^{2(n+1)\ell} \phi(x, z) dx, \quad (13)$$

where the last line follows from the periodicity of the system in x . Noting that $\hat{\phi}$ solves $-\xi^2 \nabla^2 \hat{\phi} - \hat{\phi} + \hat{\phi}^3 = 0$ up to exponentially small corrections, we may integrate Eq. (11) from $-\infty$ to ∞ in x and apply Eq. (13) in order to find

$$0 = -\partial_{zz} f(z) + 4\lambda^{-4} \int_{-\infty}^{\infty} dy' \int_0^h dz' \hat{g}(y, z, y', z') f(z'), \quad (14)$$

subject to the boundary conditions $f(0) = \alpha$ and $\frac{d}{dz} f(z) = 0$ for $z = h$. The parameter $\lambda^4 = 4\xi^2/\sigma$, while the function $\hat{g}(y, z, y', z')$ is defined as

$$\hat{g}(y, z, y', z') = \int_{-\infty}^{\infty} dk_y \frac{e^{ik_y(y-y')}}{2\pi h k_y^2} + 2 \sum_{k_z} \int_{-\infty}^{\infty} dk_y \frac{e^{ik_y(y-y')} \cos(k_z z) \cos(k_z z')}{2\pi h (k_y^2 + k_z^2)}. \quad (15)$$

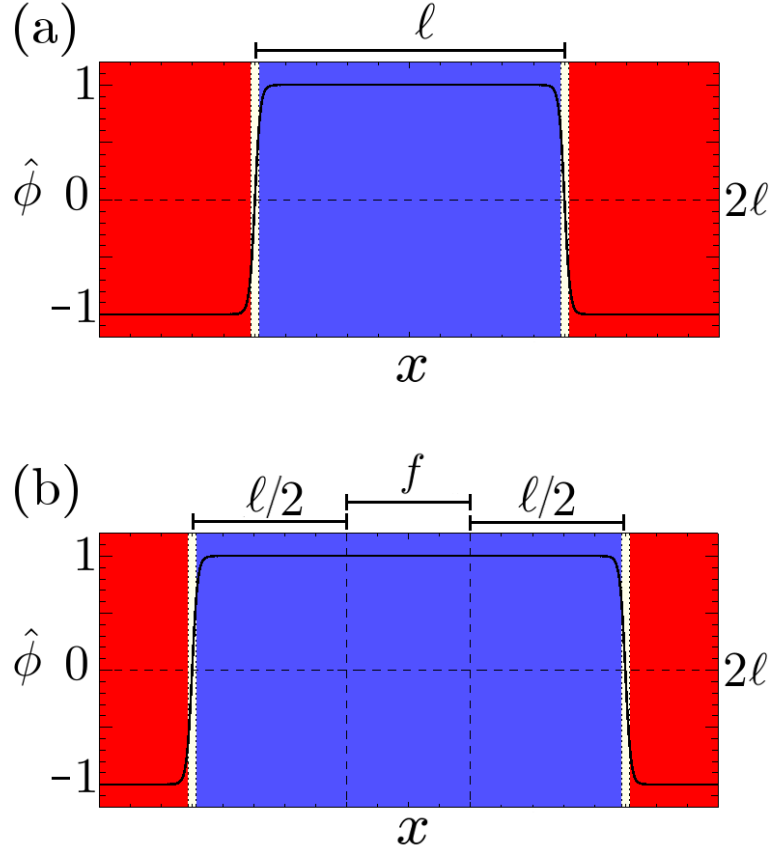


Figure 5. The function $\hat{\phi}$ [cf. Eq. (1)] as a function of x for fixed z . In the top panel, $f = 0$; in the bottom panel, $f = \ell/5$. The asymptotic behavior of $\hat{\phi}$ as $x \rightarrow \ell$ allows us to define $f \approx (1/2) \int_0^{2\ell} \hat{\phi}(x, z) dx$

Equation (14) can be solved by applying $\partial_y^2 + \partial_z^2$ to Eq. (14) and noting that $(\partial_y^2 + \partial_z^2)\hat{g}(y, z, y', z') = -\delta(y - y')\delta(z - z')$, where $\delta(z)$ is the Dirac delta function. Since f does not depend on y , this yields a fourth order, linear ordinary differential equation with a general solution of the form

$$f(z) = A_1 e^{z/\lambda} \cos(z/\lambda) + A_2 e^{z/\lambda} \sin(z/\lambda) + A_3 e^{-z/\lambda} \cos(z/\lambda) + A_4 e^{-z/\lambda} \sin(z/\lambda). \quad (16)$$

Inserting this solution into Eq. (14) and applying integration by parts to the nonlocal term yields the two constraints

$$\int f(z) dz = 0 \quad z = 0, h, \quad (17)$$

where the integral is interpreted as an indefinite integral with the arbitrary constant set to zero. Letting $F(z) = \int f(z) dz$, we find a system of four algebraic equations that determine the A_j (and consequently f):

$$\begin{aligned} F(0) &= 0, & F(h) &= 0, \\ f(0) &= a, & \partial_z f(z)|_{z=h} &= 0. \end{aligned} \quad (18)$$

If we define the interfaces to be located at the points where $\hat{\phi} = 0$, then Eqs. (1), (16), and (18) imply that the interface positions are given by Eqs. (4) and (5).

5. DISCUSSION

In this section we discuss extensions and limitations of our analysis, as well as open questions.

We first note that the approach of Sec. 4 can be generalized to templates in which the chemoepitaxial stripes exhibit peristaltic oscillations (meaning that adjacent stripe boundaries are 180° out of phase).[†] In particular, one may still define f as an integral of $\hat{\phi}$ in such a way that the former becomes a function of y and z (as opposed to just z). It is then possible to recast the PDE for $\hat{\phi}$ into a constant coefficient, fourth order linear PDE $f(y, z)$ which can be solved exactly. We are currently preparing a manuscript on this result.

Our approach does not consider the effects of pitch multiplication. In proposed applications of BCP directed self-assembly, template features are spaced with a periodicity $2n\ell$, where $n > 1$ is the pitch multiplication factor. The BCPs then assemble into microdomains over top of both the templated and non-templated parts of the substrate, effectively increasing the density of lines by a factor of n .⁴ From a modeling perspective, a key task is to determine the appropriate boundary conditions for the microdomains that self-assemble over the non-templated sections of the substrate. We speculate that $\partial_z \phi_{z=0}$ is an appropriate condition since we impose this restriction at the neutral top-coat interface, i.e. where neither polymer species preferentially wets the surface.

Our analysis also *assumes* that the monomer density has a form given by Eq. (1). While the substrate could in principle affect the density profile (especially the interface width), we believe that our assumption does not significantly alter the derivation of f . In particular, the (approximate) identity $f(z) \approx \frac{1}{2} \int_0^{2\ell} dx \phi(x, z)$ relies on the asymptotic behavior $\hat{\phi} \rightarrow \pm 1$ near the center of each microdomain (cf. Fig. 5); this behavior should be independent of the exact functional form of $\hat{\phi}$ for any polymer melt in the SSR.

We stress that while this mean-field model provides simple expressions for the microdomain interfaces, caution should be exercised when considering systems whose half-pitch is of the order of a few nanometers. At such length scales, examination of the model parameters reveals that we push the theory to the limits of its validity. Notably, for a physical system in which $\xi = 1$ nm and $\ell = 10$ nm, we find that $a = \sqrt{3\chi}\xi/2$, which is a few tenths of a nanometer for $\chi \approx 0.1$ (corresponding to PSPDMS [poly(styrene-b-dimethylsiloxane)]).¹⁶ Since we expect that the Kuhn length is the smallest meaningful length scale in our model, it is unclear that our analysis will be valid when $a/\xi > \mathcal{O}(1)$.

6. CONCLUSION

In this work, we derive analytical formulas for the microdomain interface position and monomer density profile for a lamellar BCP system with a chemoepitaxial template consisting of straight, parallel lines; in particular, we consider the case when the width of the template lines is different from the bulk microdomain width. We also determine the length scale λ over which the substrate can affect the BCP melt. Our starting model is a version of the Leibler-Ohta-Kawasaki phase-field Hamiltonian that accounts for interactions of the polymers with the substrate and top-coat. Open questions include the generalization of our result to systems with roughness in the template and applications of pitch multiplication.

Acknowledgements

Support for PP was provided by the National Institute of Standards and Technology American Recovery and Reinvestment Act Measurement Science and Engineering Fellowship Program Award No. 70NANB10H026 through the University of Maryland, with ancillary support from the Condensed Matter Theory Center at the University of Maryland. The authors also wish to thank Dionisios Margetis and Alex Liddle for useful discussion during the preparation of this manuscript.

REFERENCES

- [1] R. Ruiz, H. Kang, F. A. Detcheverry, E. Dobisz, D. S. Kercher, T. R. Albrecht, J. J. de Pablo, and P. F. Nealey, “Density multiplication and improved lithography by directed block copolymer assembly,” *Science*, vol. 321, no. 5891, pp. 936–939, 2008.
- [2] F. A. Detcheverry, G. Liu, P. F. Nealey, and J. J. de Pablo, “Interpolation in the directed assembly of block copolymers on nanopatterned substrates: Simulation and experiments,” *Macromolecules*, vol. 43, no. 7, pp. 3446–3454, 2010.

[†]Peristaltic oscillations are also referred to as line-width roughness.

- [3] P. A. Rincon Delgadillo, R. Gronheid, C. J. Thode, H. Wu, Y. Cao, M. Somervell, K. Nafus, and P. F. Nealey, "All track directed self-assembly of block copolymers: process flow and origin of defects," pp. 83230D–83230D–9, 2012.
- [4] J. Y. Cheng, C. T. Rettner, D. P. Sanders, H.-C. Kim, and W. D. Hinsberg, "Dense self-assembly on sparse chemical patterns: Rectifying and multiplying lithographic patterns using block copolymers," *Advanced Materials*, vol. 20, no. 16, pp. 3155–3158, 2008.
- [5] K. C. Daoulas, M. Muller, M. P. Stoykovich, H. Kang, J. J. de Pablo, and P. F. Nealey, "Directed copolymer assembly on chemical substrate patterns: A phenomenological and single-chain-in-mean-field simulations study of the influence of roughness in the substrate pattern," *Langmuir*, vol. 24, no. 4, pp. 1284–1295, 2008. PMID: 18067336.
- [6] G. M. Perera, C. Wang, M. Doxastakis, R. J. Kline, W. li Wu, A. W. Bosse, and G. E. Stein, "Directed self-assembly of lamellar copolymers: Effects of interfacial interactions on domain shape," *ACS Macro Letters*, vol. 1, no. 11, pp. 1244–1248, 2012.
- [7] P. N. Patrone and G. M. Gallatin, "Modeling line edge roughness in templated, lamellar block copolymer systems," *Macromolecules*, vol. 45, no. 23, pp. 9507–9516, 2012.
- [8] T. Ohta and K. Kawasaki, "Equilibrium morphology of block copolymer melts," *Macromolecules*, vol. 19, no. 10, pp. 2621–2632, 1986.
- [9] L. Leibler, "Theory of microphase separation in block copolymers," *Macromolecules*, vol. 13, no. 6, pp. 1602–1617, 1980.
- [10] C. Forrey, K. G. Yager, and S. P. Broadaway, "Molecular dynamics study of the role of the free surface on block copolymer thin film morphology and alignment," *ACS Nano*, vol. 5, no. 4, pp. 2895–2907, 2011.
- [11] Q. Wang, "Symmetric diblock copolymers in nanopores: Monte carlo simulations and strong-stretching theory," *The Journal of Chemical Physics*, vol. 126, no. 2, p. 024903, 2007.
- [12] Q. Wang, S. K. Nath, M. D. Graham, P. F. Nealey, and J. J. de Pablo, "Symmetric diblock copolymer thin films confined between homogeneous and patterned surfaces: Simulations and theory," *The Journal of Chemical Physics*, vol. 112, no. 22, pp. 9996–10010, 2000.
- [13] G. H. Fredrickson, "Computational field theory of polymers: opportunities and challenges," *Soft Matter*, vol. 3, pp. 1329–1334, 2007.
- [14] A. W. Bosse, E. K. Lin, R. L. Jones, and A. Karim, "Interfacial fluctuations in an ideal block copolymer resist," *Soft Matter*, vol. 5, pp. 4266–4271, 2009.
- [15] A. W. Bosse, "Phase-field simulation of long-wavelength line edge roughness in diblock copolymer resists," *Macromolecular Theory and Simulations*, vol. 19, no. 7, pp. 399–406, 2010.
- [16] Y. S. Jung, J. B. Chang, E. Verploegen, K. K. Berggren, and C. A. Ross, "A path to ultranarrow patterns using self-assembled lithography," *Nano Letters*, vol. 10, no. 3, pp. 1000–1005, 2010. PMID: 20146429.